JTTEE5 12:350-359

Peer Reviewed

Net Shape Nanostructured Aluminum Oxide Structures Fabricated by Plasma Spray Forming

Arvind Agarwal, Tim McKechnie, and Sudipta Seal

(Submitted 15 March 2002; in revised form 19 August 2002)

The plasma spray technique has been used by several researchers to deposit nanostructured ceramic coatings, but there is no available literature discussing how to fabricate a bulk, freestanding nanostructured component by such a technique. In the current study, net shape nanostructured Al_2O_3 structures have been fabricated using the plasma spray technique. A detailed characterization of the spray-formed Al_2O_3 structure has been performed using x-ray diffraction (XRD), scanning electron microscopy (SEM), transmission electron microscopy (TEM), and microhardness measurements. This study validates the feasibility of rapid fabrication of freestanding, near net shape nanostructured Al_2O_3 components of larger size by plasma spray forming technique. Plasma spray parameters were controlled with a proprietary cooling technique to retain a large fraction of nanosize Al_2O_3 powder particles in the spray deposit. Partially melted nanosize Al_2O_3 particles were trapped between the fully melted coarser, micrometer size Al_2O_3 grains. It was found that densification of the spray deposit has been dominated by both solidification and solid-state sintering. This study proves that a variety of nanostructured materials and their combinations can be fabricated to near net shapes by espousing a similar processing approach.

Keywords aluminum oxide, densification, nanostructured, near net shapes, spray forming

1. Introduction

The presence of nanosize particles and grains in materials results in a significant increase in the mechanical properties such as tensile strength, fracture toughness, hardness, and wear resistance. The significance of nanosize grains has been known to the materials community for a long period of time. However, an increased effort to synthesize nanostructured metals, ceramics, composites, and coatings has been seen only in the last few years.[1-4] Several synthesis techniques such as sol-gel synthesis, chemical vapor deposition, electron beam evaporation, and plasma-assisted techniques have been adopted to process nanostructured materials.[5-9] The plasma spray technique is one such method that has been used by several researchers to deposit nanostructured coatings such as WC, Cr_3C_2, Al_2O_3-TiO_2, ZrO_2.[3-4,9-12] However, these studies have been restricted to small size coupons and samples. There is no available literature that discusses how to fabricate a bulk, freestanding nanostructured component by plasma spraying. In the current work, freestanding, net shape nanostructured Al_2O_3 structures have been produced using a plasma spray technique. The addition of nanosize alumina dispersions results in an increase in the fracture toughness and thermal shock of the conventional alumina ceramics.[13] Nanoalumina-dispersed composites find a wide variety of applications including use in the electrical industry as arc tubes.[14] A detailed characterization of the spray-formed alumina structure has been performed using x-ray diffraction (XRD), scanning electron microscopy (SEM), transmission electron microscopy (TEM), and microhardness measurements.

1.1 Near Net Shape Processing

Near net shape processing using the plasma spraying technique involves simultaneous melting of powder and accelerating the molten particles for deposition on a rotating mandrel or substrate.[15,16] Figure 1 shows the schematic of plasma spray forming technique. As shown in the figure, the nozzle creates an arc that ionizes a gas stream forming the plasma with extremely high temperatures. Powders are fed into the plasma where they melt and are accelerated to supersonic speeds. The molten particles are directed toward a rotating mandrel where they deposit and rapidly cool, forming the desired shape. The spray-deposited structure is built up on the surface of the mandrel, which has the negative figure of the desired shape, and is then removed from the mandrel, usually by making use of the large difference in thermal expansion between the two components. A wide variety of complex shapes and configurations can be made using such a technique.[16-18] The process lends itself especially to refractory metals and ceramics, which can be brittle at room temperature and hard to machine. The process results in the very effective use of precursor materials because there is minimal waste and parts are sprayed to near net shape, requiring little final machining. The density of the deposited materials depends largely on the

Arvind Agarwal (currently at Department of Mechanical and Materials Eng., Florida International University, Miami, FL 33174) and **Tim McKechnie**, Plasma Processes Inc., Huntsville, AL 35811; and **Sudipta Seal**, Advanced Materials Processing & Analysis Center, Department of Mechanical, Materials and Aerospace Engineering, University of Central Florida, Orlando, FL 32816. Contact e-mail: agarwala@fiu.edu.

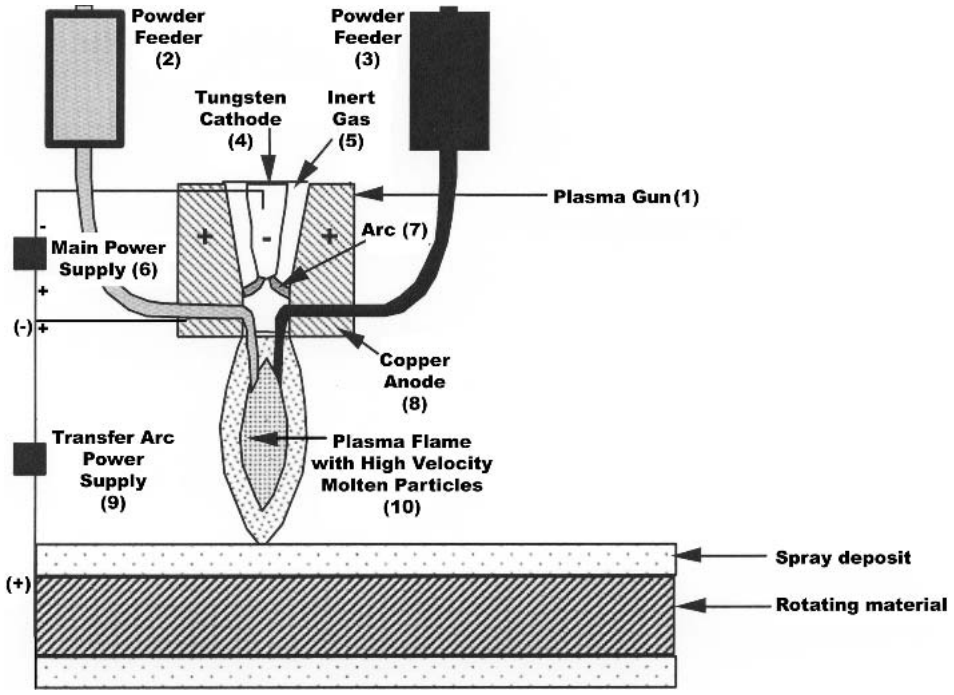

Fig. 1 Plasma-spray forming illustration: An arc ionizes a gas stream of argon and hydrogen to form the plasma into which powders are fed. Powder material is heated and accelerated to form a coating or structure on a rotating mandrel, which is later removed. The cylindrical mandrel shown can be replaced with more complex shape.

plasma velocity, which controls the time that the particles are exposed to the heating zone and the kinetic energy with which they impact the rotating mandrel. The plasma gun and the mandrel are computer controlled, allowing fabrication of complex shapes. The high temperature of the plasma implies that virtually any material that can be melted is suitable for spraying to controlled thickness and geometries. The key to develop freestanding nanostructured materials lies in the processing technique such that nanostructure is retained without significant grain growth. It can be achieved by optimum control on plasma parameters, powder feedstock, and the substrate temperature.

2. Experimental

2.1 Powder Feedstock

Commercially available aluminum oxide powder (99.8% pure) in the 15-45 μm particle size range was procured from Saint Gobain Ceramics Materials (Worcester, MA) and nanosize aluminum oxide powder (99.9% pure) was obtained from Nanophase Technologies Corporation (Romeoville, IL). Micrometer and nanosize powders were mixed at a 60:40 wt.% ratio, respectively. The dual size powder particles were thoroughly mixed in a rotating ball mill for 24 h. Alumina balls were used for milling to avoid any contamination of the powder mixture. The mixed powder was characterized using SEM to observe the degree of mixing. A homogenous mixing of the dual size alumina powder was achieved that is evident from the SEM micrograph shown in Fig. 2(a). Micrometer size alumina particles are angular in shape, whereas nanosize alumina particles are spherical agglomerates up to 20 μm diameter. Figure 2(b) is a high magnification SEM micrograph showing fine nanosize powder on the surface of a micrometer size powder particle. It was envisaged that a mixture of nanosize and micrometer size powder will enable easier flow of feedstock powder in the plasma flame as it is extremely difficult to flow nanosize powder only.[9]

2.2 Mandrel for Plasma Spray Forming

As shown in Fig. 1, a mandrel is required as the substrate for the spray deposition. The powder particles exiting from the plasma are deposited on the rotating mandrel and acquire the same shape as the mandrel. For the current study, a tapered 6061 aluminum mandrel (Fig. 3) was used. The mandrel was 100 mm in height, 62 mm in diameter (bottom), and tapers to 57 mm diameter at top (Fig. 3b). The design criterion of this mandrel was driven by the requirements to fabricate lightweight cylindrical x-ray mirrors by replication technique for the next generation space-based telescope.[19] The details of the mandrel design have been mentioned elsewhere in detail.[19] The machined mandrel had a surface finish of 0.5 μm. No surface preparation was performed on the as-machined surface. A smoother mandrel surface finish was essential to assist the separation of the spray-deposited material to yield a freestanding nanostructured component. The mandrel was thoroughly cleaned and rinsed in acetone prior to plasma spraying.

2.3 Plasma Spray Forming

Plasma spraying of the dual size mixed alumina powder was carried out using a Praxair Surface Technologies (Indianapolis, IN) SG 100 plasma spray system. Argon was used as the primary

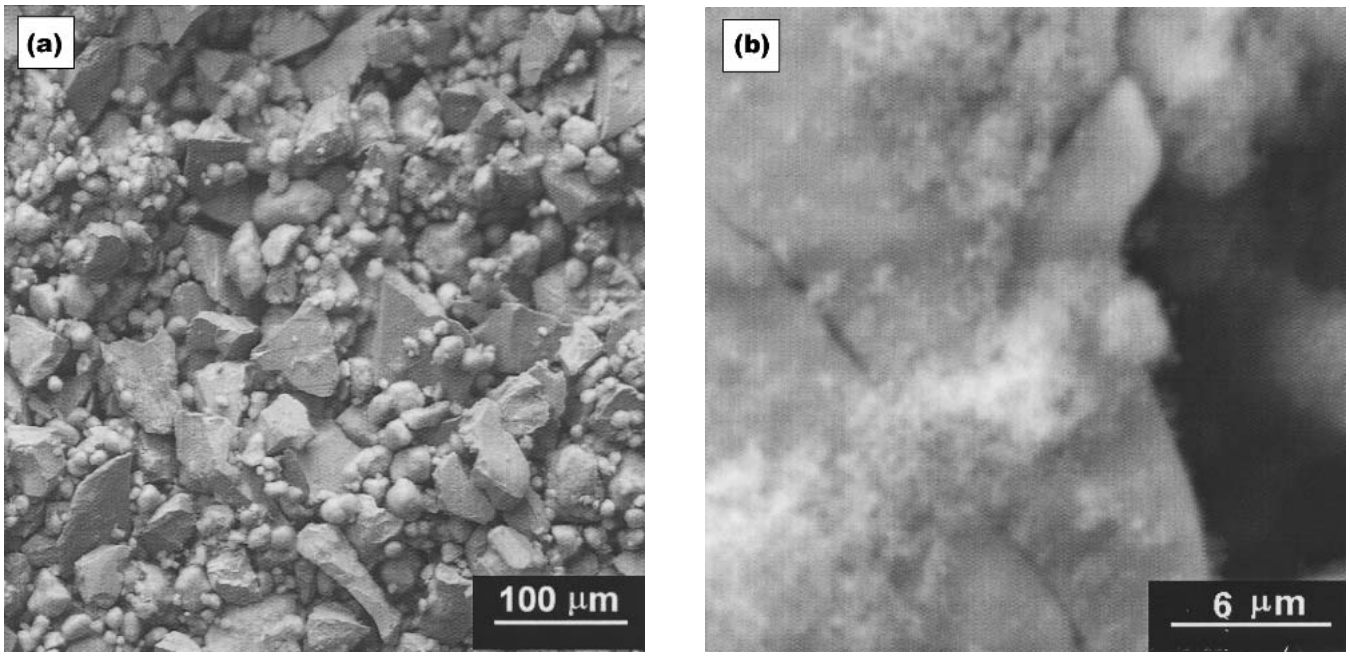

Fig. 2 SEM micrographs showing **(a)** homogenous mixture of micrometer and nanosize alumina powder particles and **(b)** nanosize powder particles on the surface of a micrometer size alumina particle

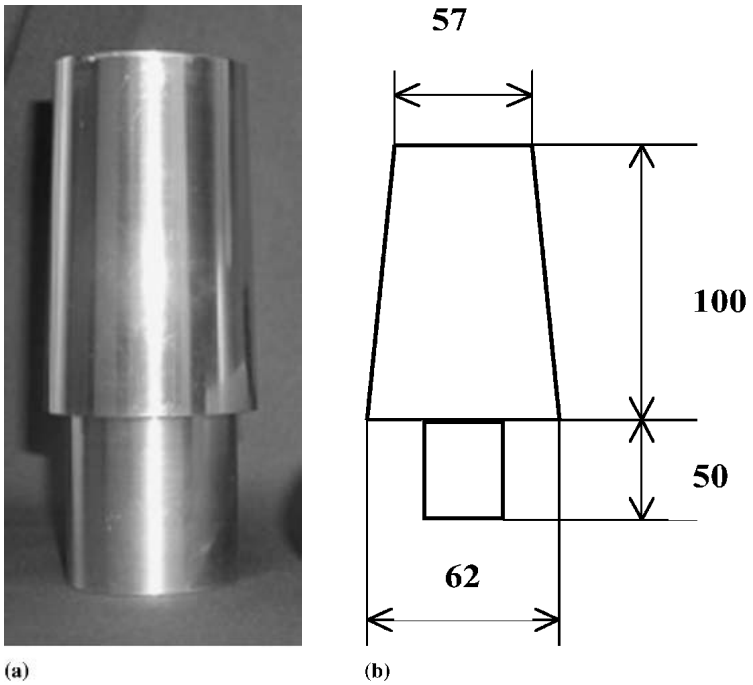

Fig. 3 **(a)** 6061 aluminum mandrel for spray forming, nanostructured alumina components. **(b)** Schematic illustration and dimension of the tapered mandrel. All dimensions are in millimeters. Tapered area was used as substrate to spray-form freestanding nanostructured alumina components

gas and helium as the secondary gas. A representative set of plasma spray parameters are listed in Table 1. Plasma parameters were controlled to minimize the coarsening and melting of nanosize powders. In addition, a proprietary cooling technique was used to actively cool the mandrel. Such active cooling increases the cooling rates and prevents coarsening of the nanosize grains in the spray deposit. Aluminum oxide coatings were spray deposited on several mandrels to a coating thickness of 300-500 μm. After spray deposition, mandrels were cooled with liquid nitrogen to facilitate the release of the spray-formed alumina shell due to mismatch between coefficients of thermal expansion (CTE). The CTE value for 6061 aluminum is 25 (10^{-6}/K),

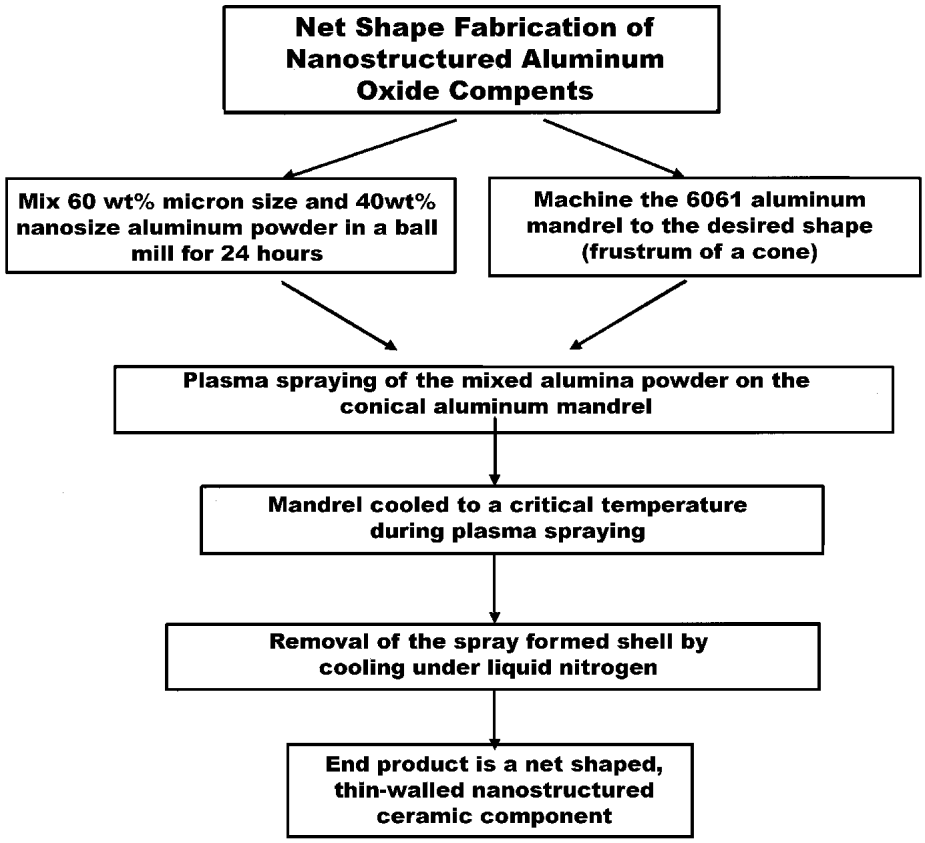

Fig. 4 Process flow chart for fabrication of nanostructured alumina components by plasma spraying

Table 1 Plasma Spray Parameters for Fabrication of Nanostructured Alumina Components

Parameter	Value
Current (amperes)	800
Voltage (volts)	35
Primary gas (argon) flow rate (SLPM/SCFH)	75/158
Standoff distance (mm)	75
Powder feed rate (g/h)	600-900
Rotational speed of the substrate (rpm)	25
Temperature of the substrate	Proprietary

whereas alumina has a CTE of 7 (10^{-6}/K).[18] The cooling was performed critically to avoid cracking of the ceramic (alumina) coating due to thermal shocks. Figure 4 summarizes the fabrication of the freestanding nanostructured alumina components by plasma spraying.

2.4 Characterization

A detailed characterization of the spray-deposited alumina was performed using several analytical tools such as XRD, SEM, TEM, and microhardness measurement. Microstructural characterization of the spray-deposited structure (phases, grain morphology) was performed using a JEOL (Peabody, MA) model 5800LV scanning electron microscope. Structural characterization for phase(s) identification was carried out on a Philips Norelco x-ray diffractometer with Cu K_α radiation operating at 30 kV and 40 mA. Microhardness measurements were performed on a LECO (St. Joseph, MI) DM 400 microhardness tester using a Vickers indenter with a normal load of 300 *g* applied for 15 s. TEM was performed to observe the retention of nanosize grains, their morphology, and physical phenomenon occurring in the spray-deposited alumina structures. A FEI (Hillsboro, OR) 200 TEM-FIB (focused ion beam) equipped with a 25-50 kV gallium liquid metal ion source (LMIS) was used for preparing thin TEM specimens from the spray-deposited alumina. A current density of ~108 A/cm^2 at the LMIS surface was approached to induce ion emission. A high beam current was used for removing large quantities of material for cleaning while a low beam current (500 pA) was used for refining the cut area for lifting out of the specimen. A FEI Technai F30 high-resolution transmission electron microscope operated at 300 kV was used for detailed microscopic analysis.

3. Results and Discussion

3.1 Net Shape Ceramic Structures

Figure 5 shows the spray-formed nanostructured alumina tapered cylindrical cones. These cones were plasma-spray-formed and released from the 6061 aluminum mandrel shown in Fig. 3(a). These tapered cylindrical alumina shells have a wall thickness of 0.4-0.6 mm. As mentioned earlier in Sec. 2.2, the driving force for such research was to fabricate lightweight x-ray mirror shells with a smooth inside finish.[19] Apart from improvement in mechanical properties, it was also anticipated that presence of nanosize alumina will improve the inside surface of the spray-

formed x-ray mirror shell. As the powder size decreases, surface detail replication increases due to more efficient packing. The inside surface of these nanostructured alumina shells was highly smooth with a surface finish of 850 nm even though it was sprayed on the as-machined mandrel.[19] It was concluded that a smoother and highly polished mandrel would further improve the inside surface finish of the replicated nanostructured alumina x-ray mirror shell.[19]

3.2 Microstructural Analysis

Figure 6(a) is the SEM micrograph showing the polished cross-section view of the spray-formed nanostructured alumina shell. The spray deposit is ~500 μm thick, homogenous, and without cracks. Figure 6(a) does not show a typical layered plasma spray structure indicating a higher degree of melting of alumina particles. However, there are few unmelted, spherical powder agglomerates present in the deposit. The black area (marked with arrow) in Fig. 6(a) appears to be porosity. However, a high magnification view of the spray deposit (Fig. 6b) indicates an alternate possibility. Some of the porosity resembles are slightly dark gray in color and indicates localized depressions or troughs (marked with arrow) 10-20 μm in size. These troughs could possibly be created by localized cracking and chipping of agglomerated nanosize alumina particles, which are also 10-20 μm in size (Fig. 2a). The microhardness indentations made on these bright gray troughs also corroborated absence of the porosity. Quantitative microscopy was performed on these SEM micrographs using Image Pro (Media Cybernetics, Carlsbad, CA) software. The black-appearing porosity of the spray deposit (Fig. 6a) was measured to be 9 vol.%. However, it should be noted that the actual porosity was less than 9 vol.% because a fraction of the measured porosity also included gray troughs. It was extremely difficult to distinguish quantitatively between the porosity and the localized gray troughs. The overall microhardness of the spray-deposited alumina was 1065 ± 73 VHN, which is higher than conventional alumina coatings in as-sprayed condition.[9] The increase in the microhardness value is attributed to the presence of nanosize grains in the structure.

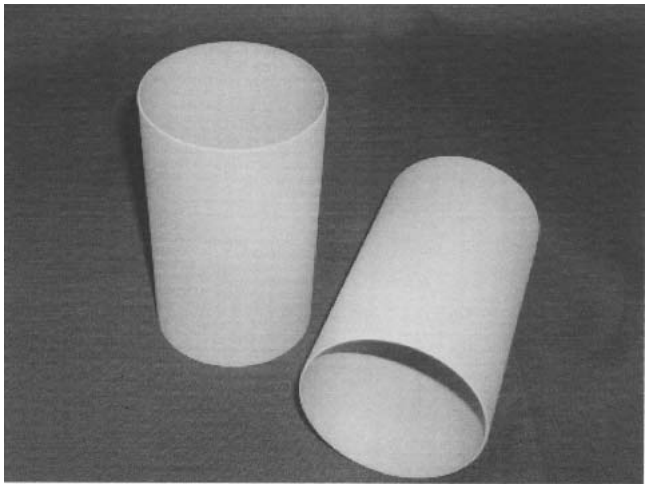

Fig. 5 Plasma-spray-formed nanostructured aluminum oxide shells with a wall thickness of 0.4-0.6 mm

3.3 Structural Characterization

The XRD spectrum of the plasma spray deposit and the starting powder mixture are shown in Fig. 7. The major phases present in the feedstock powder are stable α alumina (trigonal) and metastable γ alumina (cubic). Most of the peaks in the spray-

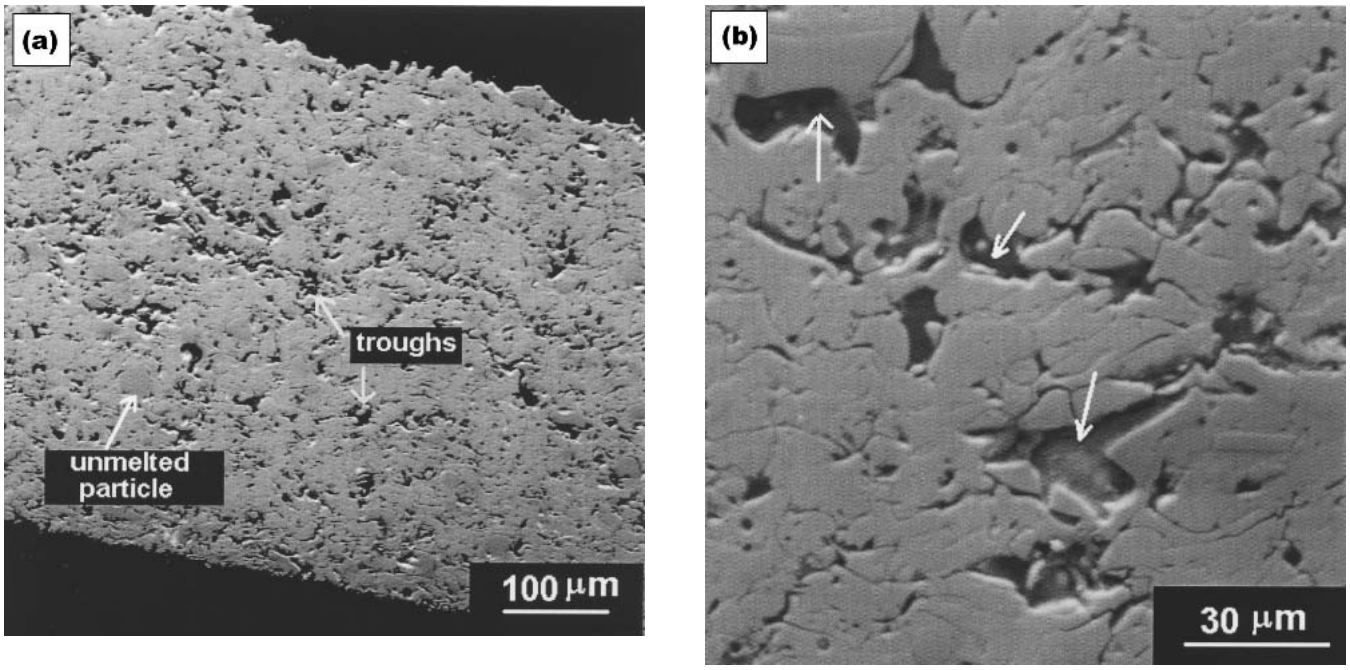

Fig. 6 **(a)** Low magnification SEM micrograph of the cross section of the spray deposit and **(b)** high magnification SEM micrograph distinguishing between porosity and localized trough

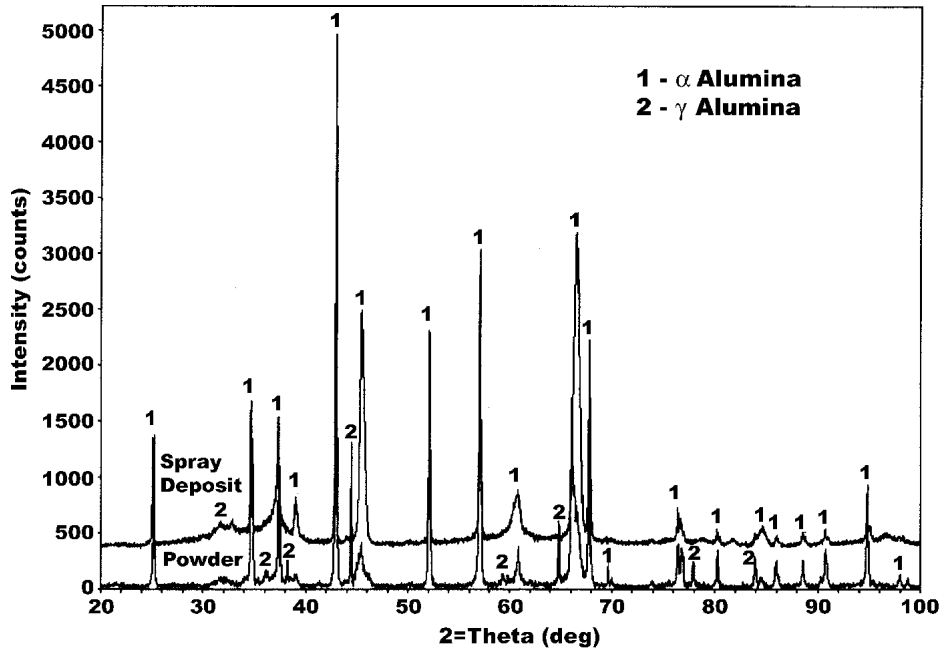

Fig. 7 XRD spectra for the feedstock mixed alumina powder and the plasma sprayed deposit

deposit structure indicate presence of α and γ phases of alumina. Aluminum oxide has several polymorphs including stable α alumina phase and a metastable γ alumina.[20] A higher degree of metastable γ alumina phase in the mixed powder is attributed to the presence of 40 wt.% nanosize powder. Nanosize alumina powder often contains a higher degree of metastable γ alumina phase due to its past processing history, which involved rapid quenching and subsequent retention of metastable phases.[20] Some portion of this metastable γ alumina phase undergoes phase transformation to α alumina phase during plasma spraying.[9] However, some of the peaks (2θ = 32, 37, 61) of the spray deposit show broadening, which insinuates overall reduction in grain size.[21] Such reduction in grain size is attributed to rapid solidification and cooling rates experienced during the plasma spraying process, which was further assisted by the proprietary cooling technique. TEM results discussed below in Sec. 3.4 further corroborate overall reduction in grain size.

In a separate study on plasma-sprayed nanostructured Al_2O_3-13 wt.% TiO_2 coatings, Shaw et al. performed the phase analysis as a function of the processing parameter (IV/Ar) where IV is the electrical power (watts) and Ar is the primary gas flow rate (SCFH).[9] An IV/Ar ratio (>310) indicated a higher degree of melting and densification by solidification, whereas a ratio <240 indicated lower melting due to relatively lower temperatures achieved.[9] The densification was dominated by sintering instead of melting for IV/Ar ratio <240. In addition, Shaw et al. predicted the following phase transformation after plasma spraying for IV/Ar <240:

α alumina (major phase in the starting powder) → traces of γ alumina + mostly α alumina (spray deposit phases)

In our current study, it can be noted from the plasma-spray parameters listed in Table 1 that the IV/Ar ratio was 180. The phases observed in the current study were similar to the work of Shaw et al. (i.e., spray deposit consists of α alumina as the major phase with traces of γ alumina). However, in contradiction to the research of Shaw et al., the densification of spray-deposited nanostructured alumina was dominated by both melting and sintering. This phenomenon is corroborated by the TEM results discussed in Sec. 3.4. Such behavior could be explained by the difference in thermal conductivity values of Al_2O_3 and TiO_2. Al_2O_3 has a thermal conductivity of 5.9 W/mK at 1000 °C, whereas TiO_2 has a thermal conductivity of 3.3 W/mK.[22] Due to higher thermal conductivity of Al_2O_3, the outside of the particle gets superheated and effectively conducts the heat to the core to cause melting.[23] Hence, it could be concluded that in the absence of TiO_2, an IV/Ar ratio of 180 would result in a relatively higher degree of melting in pure Al_2O_3. The combined densification process occurring through melting and sintering is further evident from TEM analysis discussed in Sec. 3.4.

3.4 Transmission Electron Microscopy

TEM observations assist in elucidating the physical phenomenon occurring in the spray-deposited alumina structures. Figure 8(a) shows a bright field TEM image of the overall structure of the spray-deposited nanostructured alumina. The resultant microstructure shows fully melted coarse alumina grains with columnar structure, which is a typical feature of plasma spraying. Also, a very fine nanosize grain structure is trapped between successive fully melted alumina grains (marked with arrows in Fig. 8a). This fine structure is not a resolidified structure, but densification has occurred due to the sintering effect at the edges of nanosize powder agglomerates. Figure 8(b) is a SEM micrograph of the fracture surface of the 500 μm thick spray-formed alumina shell shown in Fig. 5. It clearly shows fully melted coarse alumina particles and the trapped or retained spherical

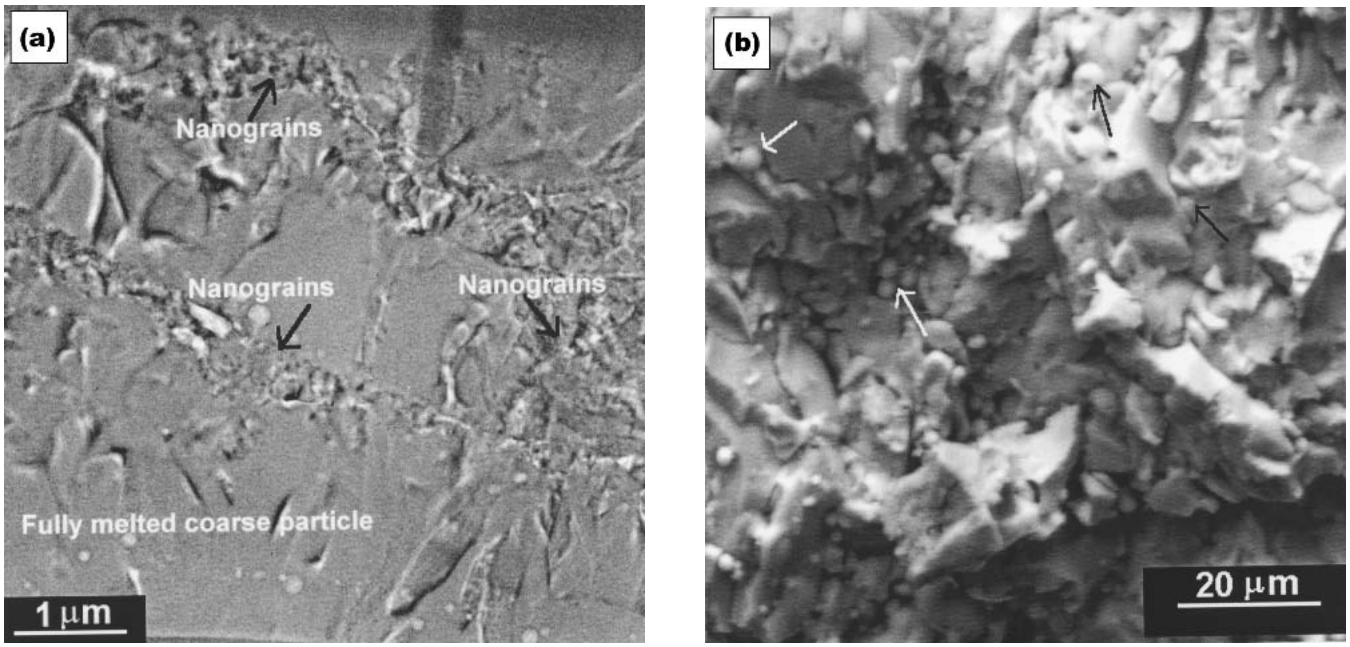

Fig. 8 **(a)** Bright field TEM micrograph showing overall microstructure of the spray-formed alumina shells and **(b)** SEM micrograph of the fracture surface of the spray-formed alumina shell

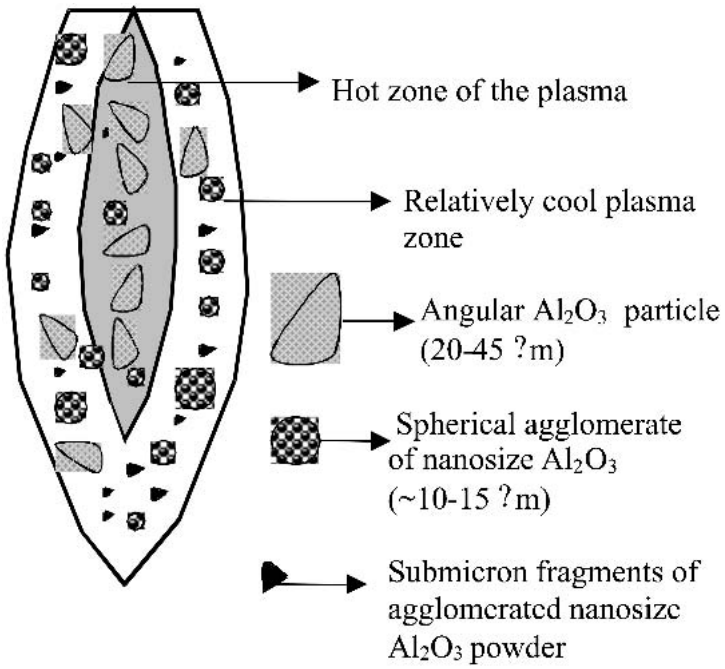

Fig. 9 A schematic of the trajectory and flow behavior of the blended powder through the plasma flame

nanosize agglomerates (marked with arrows). Figure 9 shows the schematic representation of the trajectory and flow behavior of different size Al_2O_3 powder particles through the plasma flame. A larger degree of melting occurs in micrometer-size particles because they flow coherently through the hot zone of the plasma. On the contrary, a larger fraction of nanosize powder agglomerates do not flow through the hot core of the plasma due to their smaller size. Hence, they are partially melted and trapped between the coarser particles (Fig. 8a,b). The plasma was not so hot such that it fully melts and resolidified the entire nanosize powder. Some fraction of the nanosize agglomerates in the feedstock powder has also melted in the plasma flame, but a larger

fraction of nanosize particles has been retained as a partially melted or sintered structure trapped between the coarser grains and particles. Additionally, few of the larger (10-20 μm size) nanosize agglomerates that pass though the hot core of the plasma flame undergo "explosion" resulting in a large number of tiny particles.[3] The nanometer grain size of these particles has been retained. Densification in these nanosize agglomerates occur via solid-state sintering. Densification of nanosize particles through sintering is evident from Fig. 10, which shows a highly magnified view of the structure within nanograins. It shows nanosize grain structure with necking and rounded pores (marked P), which are the features of different stages of solid-state sintering.[24] The rounded pores vary from 50-100 nm in size. Such pore rounding occurs at the advanced stages of sintering. A high magnification view of the fine structure trapped between fully melted coarse grains is presented in Fig. 11(a). It shows fine alumina grains ≤100 nm, which corroborates a high degree of retention of nanosize structure after plasma-spray forming. The selected area diffraction (SAD) pattern shows a spotty ring pattern with few bright spots (Fig. 11b). The spotty ring pattern is attributed to the presence of extremely fine (nanosize) grains, whereas bright spots arise from reflection from several planes.

Figure 12(a) shows a TEM micrograph with multiple features that include nanosize grains varying between 25-200 nm, rounded porosity due to sintering (marked with P), and substructure within a 200 nm grain (marked with arrow). The development of substructure within a nanosize grain suggests phase transformation occurring during plasma spraying. Figure 12(b) shows a high-resolution TEM image with nonspherical particles of 10-20 nm size (surrounded by black lines). The lattice fringes within these particles are oriented in various directions suggesting lack of any preferred orientation relationship between the nanosize grain and the substructure. These nonspherical particles could be one of the several polymorphs or phases of Al_2O_3, which might have transformed during plasma spraying.[21] X-ray analysis indicated γ Al_2O_3 as the only metastable phase in the spray-deposited nanostructured alumina (Fig. 7). These nonspherical particles could possibly be γ Al_2O_3; however, no SAD analysis was performed to characterize these nonspherical phases.

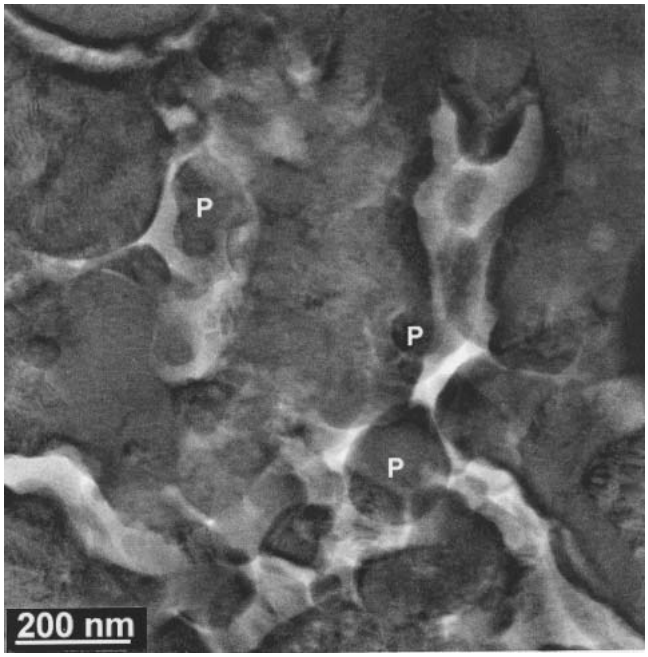

Fig. 10 Bright field TEM micrograph showing solid-state sintering occurring in the plasma-sprayed nanostructured alumina

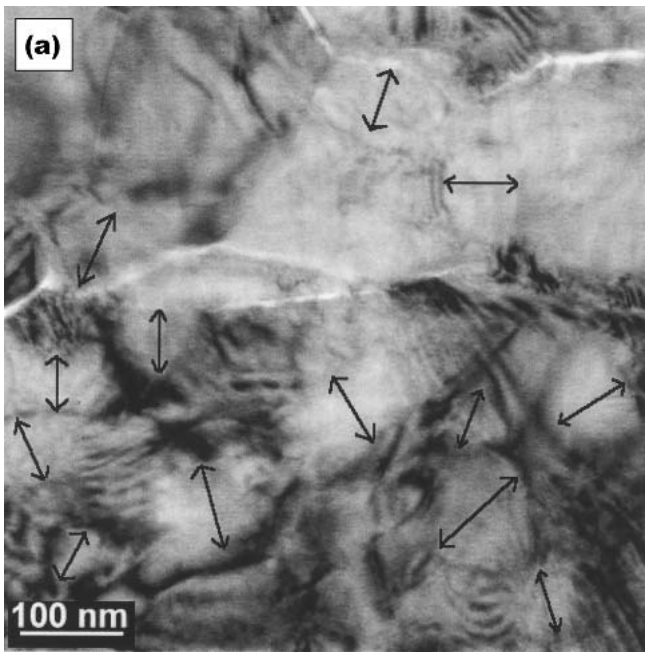

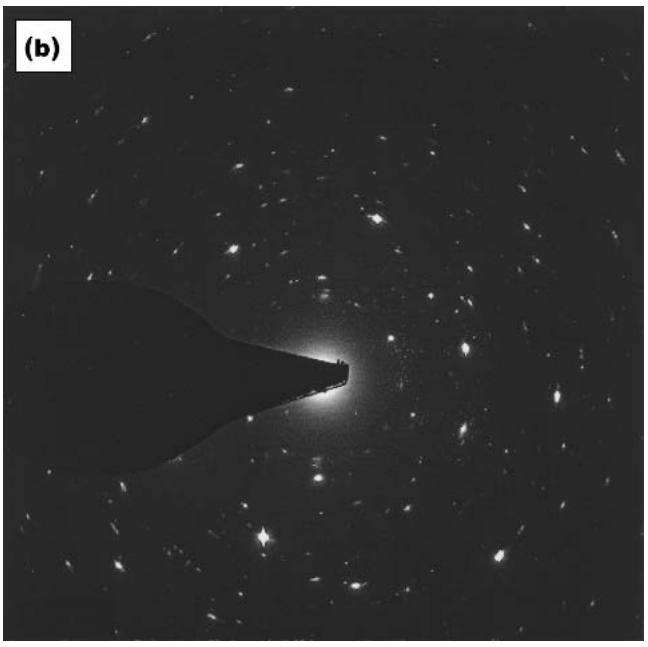

Fig. 11 **(a)** Bright field TEM micrograph showing nanosize grains in the plasma-sprayed nanostructured alumina and **(b)** corresponding SAD pattern showing spotty rings and some bright reflections

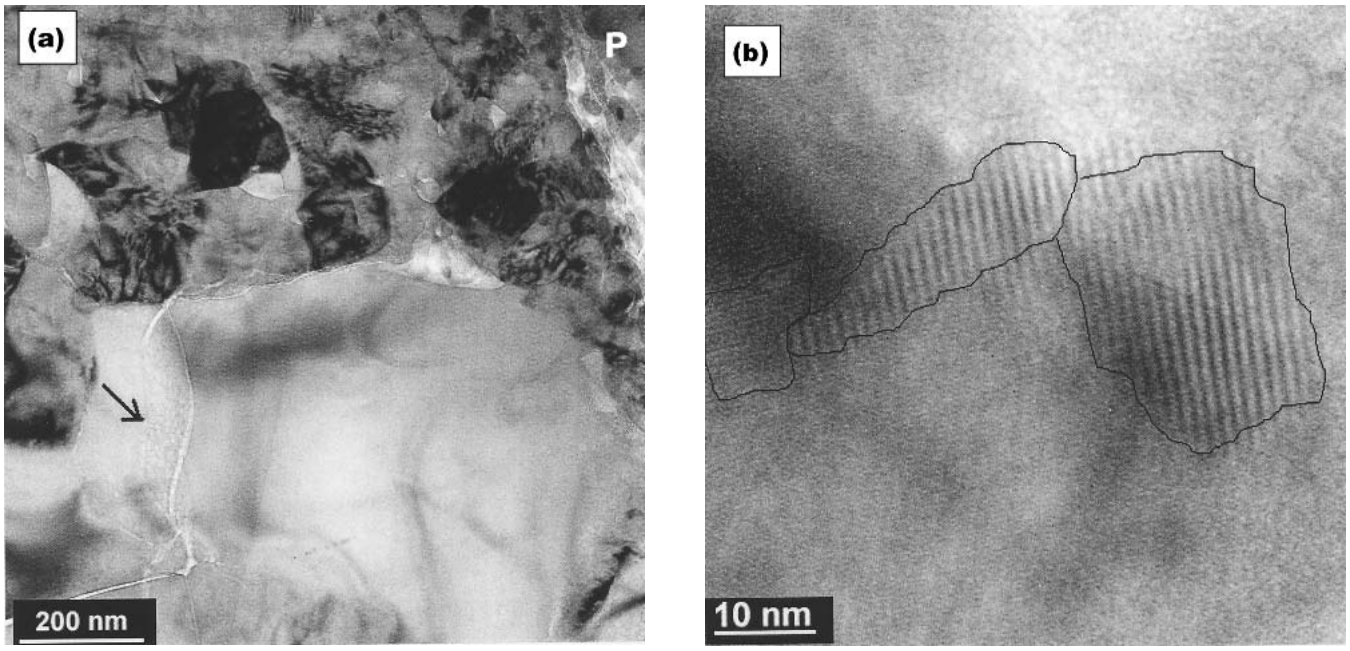

Fig. 12 Bright field TEM micrographs showing **(a)** multiple features such as nanosize grains, rounded pores due to sintering, and subdomains within a nanosize grain and **(b)** lattice fringes of nonspherical particles in various directions

4. Conclusions

- Plasma spray forming technique has successfully been used to fabricate freestanding, near net shape nanostructured Al_2O_3 component of large size.
- Plasma spray parameters were controlled with an innovative proprietary cooling technique to retain a large fraction of nanosize Al_2O_3 powder particles in the spray deposit.
- Nanosize particles have been partially melted and trapped between the fully melted coarser (micrometer size) Al_2O_3 grains. Densification of the spray deposit has been dominated by both solidification and solid-state sintering.
- Nanosize metastable Al_2O_3 phase formation occurred during plasma spraying due to rapid cooling rates associated with the process.
- A similar processing technique can be adopted for rapid fabrication of near net shapes of a variety of nanostructured materials and their combinations by suitable powder treatment and plasma spray parameters.

Acknowledgments

The authors wish to express their sincere appreciation to Ms. P. Kadolkar and Dr. N.B. Dahotre at The Center for Laser Applications, The University of Tennessee, Knoxville, for assistance with XRD analysis. The authors acknowledge financial support from the NASA Goddard Space Flight Center (Contract No. NAS5-0008) for this work.

References

1. F. Audebert, H. Sirkin, and A.Garcia Escorial: "Aluminum-Base Al-Fe-Nb Amorphous and Nanostructured Alloys," *Scr. Mater.,* 1997, *36*(4), pp. 405-10.
2. L. Cao, Y.Yuan, and L. Fu: "Preparation of Nanostructured Composites of TiN-Ni," *J. Mater. Sci. Lett*. 1996, *15*(10), pp. 849-50.
3. R.S. Lima, A. Kucuk, U. Senturk, and C.C. Berndt: "Properties and Microstructures of Nanostructured Partially Stabilized Zirconia Coatings," *J. Therm. Spray Technol.,* 2001, *10*(1), pp. 150-52.
4. J. He, M. Ice, J.M. Schoenung, D.H. Shin, and E.J. Lavernia: "Thermal Stability of Nanostructured Cr_3C_2-NiCr Coatings," *J. Therm. Spray Technol.,* 2001, *10*(2), pp. 293-300.
5. S. Seal and S. Shukla: "Cluster Size Effect Observed for Gold Nanoparticles Synthesized by Sol-Gel Technique as Studied by X-ray Photoelectron Spectroscopy," *Nanostructured Mater.*, 1999, *11*(8), pp. 1181-93.
6. G. Skandan: "Processing of Nanostructured Zirconia Ceramics," *Nanostructured Mater*., 1995, *5*(2), pp. 111-26.
7. Y. Xie: "Preparation of Ultrafine Zirconia Particles," *J. Am. Ceram. Soc*. 1999, *82*(3), pp. 768-70.
8. J. Karthikeyan, C.C. Berndt, J. Tikkanen, J.Y. Wang, A.H. King, and H. Herman: "Nanomaterial Powders and Deposits Prepared by Flame Spray Processing of Liquid Precursors," *Nanostructured Mater.,* 1997, *8*(1), pp. 61-74.
9. L.L. Shaw, D. Goberman, R. Ren, M. Gell, S. Jiang, Y. Wang, T.D. Xiao, and P.R. Strutt: "The Dependency of Microstructure and Properties of Nanostructured Coatings on Plasma Spray Conditions," *Surf. Coat. Technol.*, 2000, *130*, pp. 1-8.
10. Y. Zhu, K. Yukimura, C. Ding, and P. Zhang: "Tribological Properties of Nanostructured and Conventional WC-Co coatings Deposited by Plasma Spraying," *Thin Solid Films,* 2001, *388*, pp. 277-82.
11. Y. Wang, S. Jiang. M. Wang, S. Wang, T.D. Xiao, and P.R. Strutt: "Abrasive Wear Characteristics of Plasma Sprayed Nanostructured Alumina/Titania Coatings," *Wear,* 2000, *237*, pp. 176-85.
12. H. Chen and C.X. Ding: "Nanostructured Zirconia Coating Prepared by Atmospheric Plasma Spraying," *Surf. Coat. Technol.*, 2002, *150*, pp. 31-36.
13. G. Li, A. Jiang, and L. Zhang: "Mechanical and Fracture Properties of Nano Al_2O_3," *J. Mater. Sci. Lett.,* 1996, *15*(19), pp. 1713-15.
14. N. Dahl: "Alumina Nano Powders Sintered," *High Tech. Ceram. News,* 1998, *10*(7), pp. 3-4.
15. A. Agarwal and T. McKechnie: "Spray Forming Aluminum Structures," *Adv. Mater. Process.*, 2001, *159*(5), pp. 44-46.
16. A. Agarwal, R. Hickman, T. McKechnie, and J.S. O'Dell: "Advances in

Near Net Shape Forming and Coating of Erosion Resistant Ultra High Temperature Materials," Tri-Service Sponsored Symposium on Advancements in Heatshield Technology, Huntsville, AL, May 10-11, 2000, US Army Aviation & Missile Command, SR-RD-PS-00-01.

17. R. Hickman, T. McKechnie, and A. Agarwal: "Net Shape Fabrication of High Temperature Materials for Rocket Engine Components," 37th AIAA/ASME/SAE/ASEE/Joint Propulsion Conference**,** Salt Lake City, Utah, 8-11 July, 2001, AIAA-2001-3435.
18. A. Agarwal, T. McKechnie, and D. Engelhaupt: "Net Shape Forming of Light Weight Optical Structures for Space Applications" in *Optics Manufacturing for Dual-Use*, Huntsville, AL, February 14-15, 2001, Aviation and Missile Research, Development and Engineering Center, RD-MG-02-01.
19. A. Agarwal and T. McKechnie: "Low Cost Fabrication Lightweight Optics, Mirrors and Benches," NASA Goddard Space Flight Center, Technical Report NAS5-0008, November 2001.
20. I. Levin and D. Brandon: "Metastable Alumina Polymorphs: Crystal Structures and Transition Sequences," *J. Am. Ceram. Soc.,* 1998, *81*(8), pp. 1995-2012.
21. B.D. Cullity: *Elements of X-Ray Diffraction*, 2nd ed., Addison Wesley, Reading, MA, 1978, pp. 281-89.
22. TAPP 2.2: *A Database of Thermochemcial and Physical Properties*, ESM Software Inc., Hamilton, OH, 1998.
23. E. Lugscheider and I. Kvernes: "Thermal Barrier Coatings: Powder Spray Process and Coating Technology" in *Intermetallic and Ceramic Coatings*, N.B. Dahotre and T.S. Sudarshan, ed., Marcel Dekker, New York, 1999, pp. 267-306.
24. R.M. German: *Sintering Theory and Practice,* John Wiley & Sons, New York, 1996, pp. 67-141.